

Nanocomposites by Melt Intercalation Based on Polycaprolactone and Organoclay

YINGWEI DI,¹ SALVATORE IANNACE,² ERNESTO DI MAIO,² LUIGI NICOLAIS^{1,2}

¹Department of Materials and Production Engineering, University of Napoli "Federico II", Piazzale Tecchio 80, 80125, Napoli, Italy

²Institute of Composite Materials and Biomaterials (IMCB-CNR), Piazzale Tecchio 80, 80125, Napoli, Italy

Received 24 July 2002; revised 16 December 2002; accepted 23 December 2002

ABSTRACT: Nanocomposites based on biodegradable polycaprolactone (PCL) and organically modified layered silicates (organoclay) were prepared by melt mixing. Their structures and properties were characterized by wide-angle X-ray diffraction, thermal analysis, and rheological measurements. The exfoliation of the organoclay was achieved via a melt mixing process in an internal mixer and showed a dependence on the type of organic modifier, the organoclay contents, and the processing temperature. The addition of the organoclay to PCL increased the crystallization temperature of PCL, but a high content of the organoclay could show an inverse effect. The PCL/organoclay nanocomposites showed a significant enhancement in their mechanical properties and thermal stability due to the exfoliation of the organoclay. The nanocomposites showed a much higher complex viscosity than the neat PCL and significant shear-thinning behavior in the low frequency range. The shear storage modulus and loss modulus of the nanocomposites also exhibited less frequency dependence than the pure PCL in the low frequency range, and this was caused by the strong interactions between the organoclay layers and PCL molecules and by the good dispersion of exfoliated organoclay platelets in the PCL. © 2003 Wiley Periodicals, Inc. *J Polym Sci Part B: Polym Phys* 41: 670–678, 2003

Keywords: polycaprolactone; organoclay; nanocomposites; mixing

INTRODUCTION

Over the past decade, polymer nanocomposites have received considerable interest as an effective method for developing new composite materials, and they have been studied widely. They are a class of hybrid materials composed of organic polymer matrices in which inorganic particles with at least one nanoscale dimension are embedded. At this scale, the inorganic fillers dramatically improve the physical and mechanical mac-

roscopic properties of polymers, even though their amount is small. Compared to pristine polymer matrices, polymer nanocomposites usually exhibit higher distortion temperatures, enhanced flame resistance, increased moduli, better barrier properties, and decreased thermal expansion coefficients.¹ The enhanced properties are presumably due to the synergistic effects of the nanoscale structure and the interaction of the fillers and polymer. Recently, special attention has been paid to the development of nanostructured composites based on thermoplastics and organically modified layered silicates (organoclay), such as montmorillonite (MMT), because of the nanoscale size of the layer thickness and the intercalation

Correspondence to: S. Iannace (E-mail: iannace@unina.it)

Journal of Polymer Science: Part B: Polymer Physics, Vol. 41, 670–678 (2003)
© 2003 Wiley Periodicals, Inc.

properties.² Therefore, the achievement of exfoliation (delamination) of these layered silicates in a polymer matrix is essential for preparing objective nanocomposites. During the early stages of development, an effective hybrid formation was conducted mostly via a solution medium.³ However, direct melt intercalation has been recognized as a promising approach more recently because it can be performed with a conventional polymer mixing or extrusion process, and it is environmentally benign as well.⁴ The commercial thermoplastics of interest to be hybridized with organoclay include styrenic polymers,^{5,6} polyolefins,^{7,8} nylons,^{9,10} and so forth.

During intercalation, the polymer chains, which are initially in an unconstrained environment, must enter the constrained environment of the narrow silicate interlayer, and this results in a decrease in the overall entropy of the polymer chains. However, the organic chains gain configurational freedom as the interlayer distance increases, and this may compensate for the entropic penalty of polymer confinement.¹¹ The interaction between the organic modifiers and the molecules of the polymer matrix will favor the intercalation process of polymer molecules into the interlayers of silicates.¹² Then, under proper processing conditions, the exfoliation of the silicate layers will be achieved. Therefore, the selection of the appropriate polymer matrix and organoclay is essential for the preparation of nanocomposites by melt mixing.

Moreover, biodegradable polymers have received much attention as materials for reducing environmental problems caused by conventional plastic wastes. The production of these polymers has been studied, and their commercial applications are growing progressively. Clay materials are environmentally friendly, naturally abundant, and economic. Therefore, making nanocomposites based on biodegradable polymers and organoclay could, on the one hand, obtain new biodegradable nanocomposites with improved properties in comparison with neat biodegradable polymers and enlarge the application fields of biodegradable polymers; on the other hand, no effect would be made on the environment. Polycaprolactone (PCL) has been a biodegradable polymer of interest for medical applications, such as drug delivery systems, since it was developed, and recently it has also been applied to the food packaging industry.¹³ As polymer–organoclay composites provide significant improvements in mechanical, thermal, and gas barrier properties and

in processability for the foam-producing process, it is expected that PCL–organoclay nanocomposites could make PCL more useful from the viewpoint of applications.

PCL nanocomposites have been made previously by monomer polymerization in solution media.^{14,15} It was reported that this nanocomposites exhibited a significant reduction in water-vapor permeability.¹⁴ Very recently, Dubois et al.¹⁶ also reported PCL nanocomposites with clay. However, the processing condition effect on the exfoliation of clay layers and the melting and crystallization behavior of the resultant nanocomposites were not studied in detail. In this article, we present the preparation of the PCL–organoclay nanocomposites by melt mixing. The dependence of organoclay intercalation and/or exfoliation on the processing conditions and type of organoclay and the thermal and rheological behavior of the resultant nanocomposites have been studied. The particular combination of PCL and organoclay was chosen because the resultant nanocomposite could have potential commercial relevance as a material for producing foam and on the basis of recent literature reports on the successful preparation of polymer–organoclay nanocomposites.

EXPERIMENTAL

Materials

PCL, under the commercial name of CAPA 680, was commercially purchased from Solvay Interlox, Ltd. (United Kingdom). The two types of organoclay used in the preparation of the nanocomposites (for comparison) were purchased from Southern Clay Products, Inc. (United States), under the commercial names of Cloisite 30B and 93A (hereafter denoted 30B and 93A, respectively) and were used as received. According to the product information from the producer, these two organoclays, consisting of the same 2:1 MMT, are organics treated differently. 30B contains a quaternary ammonium ion containing methyl tallow bis-2-hydroxyethyl, and 93A contains methyl dihydrogenated tallow ammonium as an organic modifier.

Sample Preparation

A Haake Rheomix 600 internal mixer with two roller rotors was used for the preparation of PCL/organoclay nanocomposites with different compositions. This mixer was attached to a measuring

drive unit (Haake Rheocord 9000). The processing temperatures were set at 100 and 180 °C, respectively. The rotor rotating speed and mixing time were fixed at 100 rpm and 12 min, respectively. The components were first dry-blended at predetermined compositions and subsequently melt-mixed in the mixer. After being mixed, the samples were dumped out and compressed into about 2-mm-thick plates by a calendar for further characterization.

Characterization

The wide-angle X-ray diffraction (WAXD) work was performed at the ambient temperature with a Philips X-ray generator and a Philips diffractometer (PW1710) for the evaluation of the dispersability of the organoclay layers in the PCL matrix. The X-ray beam was nickel-filtered Cu K α radiation with a wavelength of 1.54 Å, operated at a generator voltage of 40 kV and at a current of 20 mA. The diffraction intensity data were collected automatically at a scanning rate of 0.6°/min in 0.01°/s steps. The organoclay was studied as a powder, and the blends were in flat films. The basal spacing of the organoclay was estimated from the (001) peak in the WAXD pattern with Bragg's law: $d = \lambda/2 \sin \theta_{\max}$.

The thermal stability of the samples was characterized by thermogravimetric analysis (TGA) on a TGA 2950 (TA Instruments, United States) under an air atmosphere at a heating rate of 10 °C/min, from room temperature to 800 °C.

The dynamic mechanical analysis was performed with a model DMA983 dynamic mechanical analyzer (TA Instruments). The testing was carried out in the three-point bending mode at a vibration frequency of 1 Hz from 0 to 60 °C at a heating rate of 3 °C/min in a dry air atmosphere.

A differential scanning calorimetry (DSC) analysis was carried out on a DSC2910 (TA Instruments). About 10 mg of the sample was weighed very accurately in an aluminum DSC pan and placed in a DSC cell. It was heated from 20 to 100 °C at a rate of 10 °C/min under a nitrogen atmosphere. The sample was kept at 100 °C for 3 min for the elimination of the previous heat history and was subsequently cooled to 20 °C at 10 °C/min. The sample was then heated again to 100 °C at 10 °C/min. This second heating process was regarded as a melting scan for the analysis. The crystallization and melting temperatures were determined as the temperatures at the

maximum values of crystallization and melting peaks.

Dynamic rheological measurements were carried out with an advanced rheometric expansion system rheometer from Rheometric, Inc. (United States). The measurements were performed in an oscillatory shear mode with parallel-plate geometry 25 mm in diameter at 80 °C under a nitrogen atmosphere. Frequency sweeps between 0.01 and 100 rad/s were carried out at low strains (0.1–10%) shown to be within the linear viscoelastic range. Before the tests, time sweep tests were also carried out so that we could be sure that no significant thermal degradation occurred within the experimental time. Specimens were placed between the preheated plates at an experimental temperature and were allowed to equilibrate before each frequency sweep run. The obtained values were corrected to the true volume between the plates.

RESULTS AND DISCUSSION

Structure from Melt Mixing

WAXD is a conventional method for characterizing the gallery height in clay particles. As the melt intercalation process proceeds, the gallery height increases, and this results in a shift of characteristic reflections to lower angles. If complete exfoliation or delamination takes place (and in a disordered nanocomposite), no reflection peak is discernible in the X-ray diffraction pattern within a low angle range.¹⁷ The WAXD patterns of 30B and PCL/30B nanocomposites are compared in Figure 1. The primary silicate reflection at $2\theta = 5.02^\circ$ of 30B corresponds to a layer spacing of 1.76 nm. For the 2 and 5 wt % 30B nanocomposites, we did not see any noticeable peaks of 30B in the low angle range, and this confirmed the exfoliated structure of silicate layers of 30B in the PCL matrix after melt mixing. For 10 wt % 30B hybrids, a broad peak at $2\theta = 3.0^\circ$, much lower than that of pristine 30B, was observed, indicating that intercalation of 30B occurred together with some exfoliation. The results in Figure 1 show that intercalation and/or exfoliation of 30B could be accomplished by melt mixing in an internal mixer. Recently, an exfoliation mechanism for organoclay has been proposed.¹⁸ In summary, during the mixing process of the polymer matrix and organoclay, the fracturing process of the organoclay particles takes place first; that is,

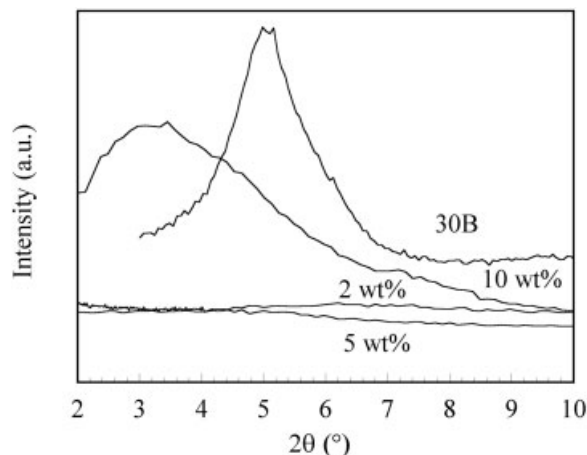


Figure 1. X-ray diffraction scans for 30B and PCL/30B nanocomposites with different weight fractions of 30B.

external platelets are subjected to dynamic high shear forces that ultimately cause their delamination from the stack of layers building the organoclay particles, and then an onion-like delamination process continues to disperse the platelets of silicate into the polymer matrix. In the PCL/30B composites, these two steps are also presumed to have taken place. As an example, Figure 2 shows the mixing torque as a function of time during the compounding process in the internal mixer for PCL/organoclay nanocomposites. For the PCL/30B system, the torque increases gradually with the mixing time, reflecting on the fracturing of the 30B particles into small aggregate, which is followed by a delamination process eventually leading to the dispersion of thin platelets

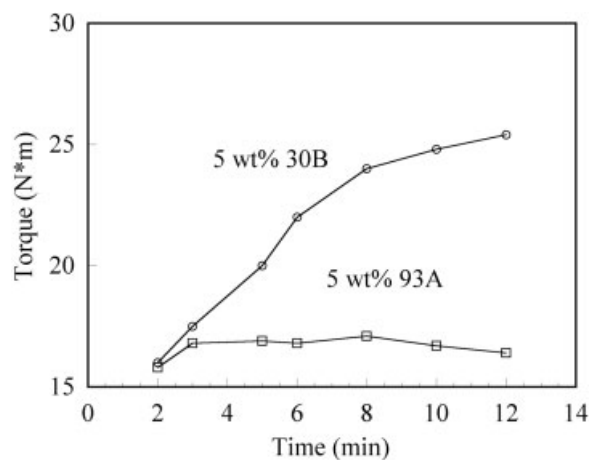


Figure 2. Mixing torque variation with the mixing time for PCL/30B and PCL/93A hybrids.

into the PCL matrix melt, as evidenced by the WAXD patterns in Figure 1. The mixing torque of PCL/93A was almost constant during the mixing period, and this suggested that the 93A particles stayed almost intact, behaving as regular filler particles; this is contrary to PCL/30B hybrids. The resultant hybrid structure for PCL/93A was examined by WAXD, and the diffractograms in Figure 3 show the almost unchanged structure of the 93A before and after the mixing process. A new broad peak appearing around $2\theta = 5.9^\circ$ indicates a partial collapse of the layered structure of 93A. The increase in the torque (also the viscosity) in Figure 2 for PCL/30B also implies that additional interactions between the hydroxyl groups in the organic modifier of 30B and the carbonyl groups in PCL are higher than those for PCL/93A between the nonpolar group of the modifier in 93A and PCL molecules. According to a previous investigation into the kinetics of polymer melt intercalation,¹¹ during the intercalation process, the polymer chains, which are initially in an unconstrained environment, must enter the constrained environment of the narrow silicate interlayer. Complete layer separation (exfoliation) depends on the establishment of very favorable polymer surface interactions needed to overcome the penalty of polymer confinement; then, with the help of proper shearing, the exfoliation structure of the silicate layers will be achieved. This has been shown by the PCL/30B nanocomposites in this study. Accordingly, we selected 30B as the organoclay for this study. The following discussion is focused only on PCL/30B nanocomposites.

However, under constant processing conditions, the organoclay content also plays an impor-

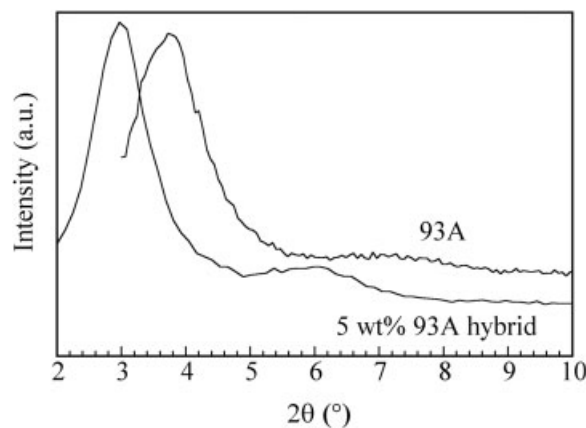


Figure 3. X-ray diffraction scans for 93A and the PCL/93A composite.

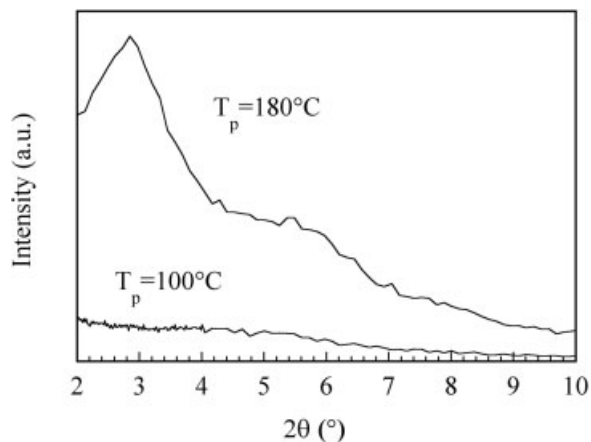


Figure 4. X-ray diffraction scans for PCL/30B (5 wt %) nanocomposites mixed at different processing temperatures (T_p).

tant role in determining the exfoliation of the organoclay layers in nanocomposites. As shown in Figure 1, for the high-content hybrid composite (10 wt %), a broad reflection at an angle lower than that of neat 30B can be observed, indicating that both intercalation and exfoliation of the organoclay exist in the PCL matrix. According to the exfoliation mechanism previously mentioned, at higher 30B contents, because of the formation of more interaction sites, which also reduce the segmental movement level, more time is needed for the fracturing and delamination steps than the lower 30B content systems require.

The mixing temperature may also influence the intercalation and/or exfoliation of organoclay. In Figure 4, the WAXD patterns of PCL/30B nanocomposites mixed at two different temperatures are compared. At a higher processing temperature (180 °C), a reflection peak can be observed at an angle lower than that of neat 30B, but no reflection peak can be observed for the nanocomposite processed at a lower temperature (100 °C). This is because the organoclay is subjected to a higher shear stress at a low processing temperature than at a high processing temperature. Accordingly, processing high interacting systems in an efficient shearing field is an important parameter in the fracturing and delamination steps of clays, leading to the formation of nanocomposite structures.

Thermal Properties

The thermal properties of PCL are affected significantly by the addition of organoclay 30B. Fig-

ure 5 presents the DSC cooling scan thermograms of PCL and PCL/30B nanocomposites. The crystallization peak temperature of PCL is 26.4 °C, whereas 2 and 5 wt % 30B additions increase this temperature up to 29.8 and 35.6 °C, respectively. At a higher 30B content (10 wt %), a slight decrease in the crystallization peak temperature compared with that of the 5 wt % 30B nanocomposite is shown at 29.2 °C; however, it is still higher than that of neat PCL. These results clearly show that the addition of a small amount of 30B to the PCL matrix results in an obvious increase in the crystallization temperature of the polymer matrix. This behavior can be explained by the assumption that the silicate layers act as efficient nucleating agents for the crystallization of the PCL matrix, causing a crystallization rate higher than that of neat PCL.⁷ This effect will be increased with increases in the organoclay contents (e.g., 2 and 5 wt % 30B nanocomposites). However, in this study, a higher content of 30B (e.g., 10 wt %) resulted in a decrease in the crystallization temperature in comparison with the temperatures for lower organoclay contents, as shown in Figure 5. This leads us to consider other factors hindering the crystallization process of the polymer matrix. Because of the strong interaction between the organic surfactant covered on the surface of the platelets of 30B and the functional groups on the main chain of PCL molecules, polymer chains attached to the platelets are partially hindered from taking part in the flow process and their crystallization process. A higher content of the organoclay will result in more interacting sites, which cause reductions in the mobility of the PCL molecules and, therefore, the

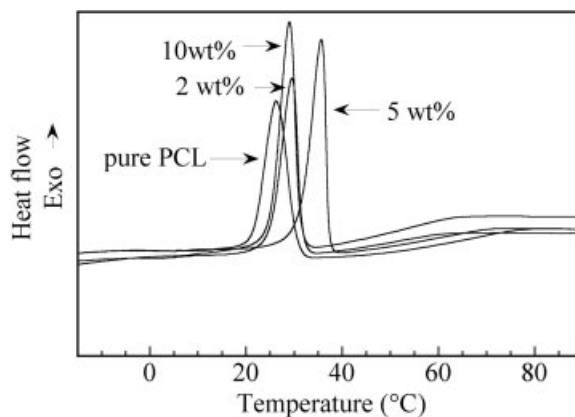


Figure 5. Crystallization exotherms of PCL and PCL/30B nanocomposites with different weight fractions of 30B.

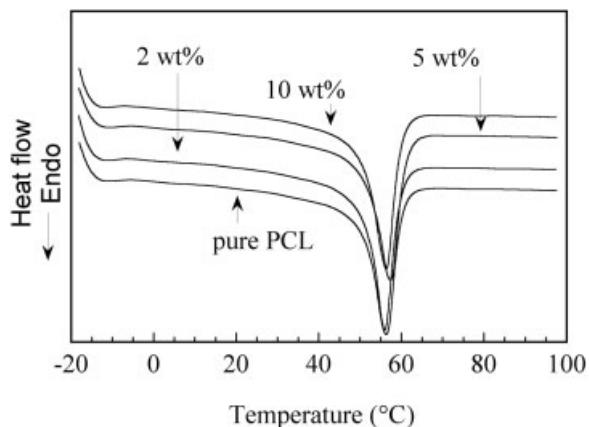


Figure 6. Melting endotherms of PCL and PCL/30B nanocomposites with different weight fractions of 30B crystallized at a 10 °C/min cooling rate.

crystallization temperature. Accordingly, the addition of the organoclay to the polymer matrix, in addition to a nucleation effect, can act as a retardant of crystallization if there is a strong interaction between the polymer matrix and organoclay. The former effect is pronounced at a lower organoclay content, and as the organoclay content is increased, the latter effect will become dominant.

In Figure 6, the melting behaviors of PCL and PCL/30B nanocomposites are shown. The melting peak temperatures of the nanocomposites are not changed significantly with respect to the pure PCL, and this indicates that the addition of 30B to PCL does not change the crystal forms and the crystal structure of PCL; that is, the melting temperature of PCL is not changed.

Figure 7 depicts the temperature dependence of the dynamic storage modulus (E') of pure PCL and PCL/30B nanocomposites from the dynamic mechanical thermal analysis tests. Over the entire temperature range, E' of the nanocomposites shows much higher values than that of pure PCL, and E' increases with increasing organoclay contents. Furthermore, the temperature dependence of E' of the nanocomposites is weaker than that of PCL; that is, E' of the nanocomposites showed a wider plateau than the pure PCL over the experimental temperature range, which was between the glass-transition temperature and melting temperature of PCL. The enhancement of the mechanical properties of PCL by the addition of the organoclay could also be attributed to the strong interaction between the organoclay 30B and PCL molecules and the good dispersion of 30B plate-

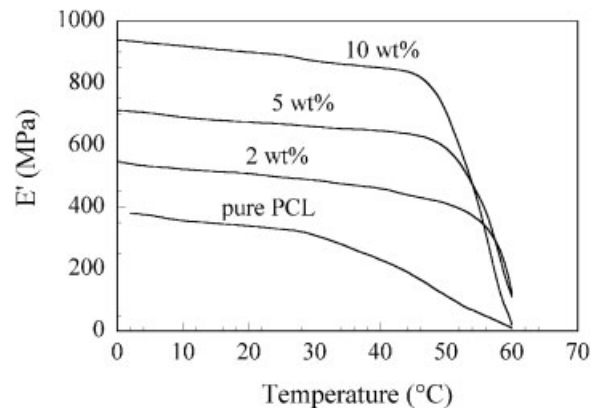


Figure 7. Temperature dependence of E' for pure PCL and PCL/30B nanocomposites with different weight fractions of 30B.

lets in the PCL matrix. Improved strength has also been observed for other polymer/clay nanocomposites and depends on the degree of intercalation of polymer chains and/or exfoliation of clay.^{19,20}

The thermal stabilities of PCL and PCL/30B nanocomposites were studied by TGA. In Figure 8, the TGA thermograms of PCL and PCL/30B nanocomposites with different compositions of 30B are compared. The onset of the thermal decomposition of the nanocomposites shifted significantly toward the higher temperature range with respect to that of PCL, and this confirms the enhancement of the thermal stability of the PCL/30B nanocomposites. An increase in the thermal stability has also been shown by other polymer/clay hybrids, such as polypropylene/clay,²¹ poly-

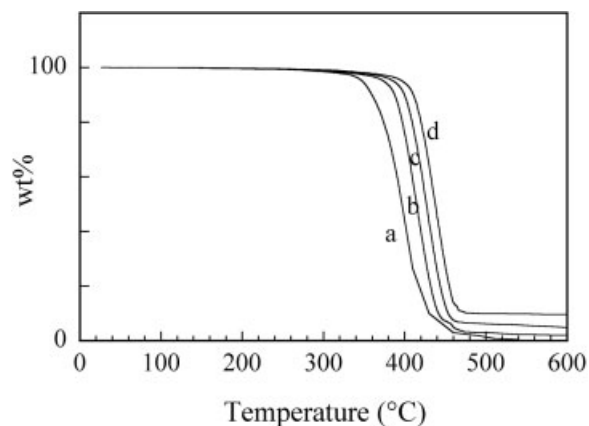


Figure 8. TGA scans for (a) PCL and (b–d) PCL/30B nanocomposites with different weight fractions of 30B (2, 5, and 10 wt %, respectively).

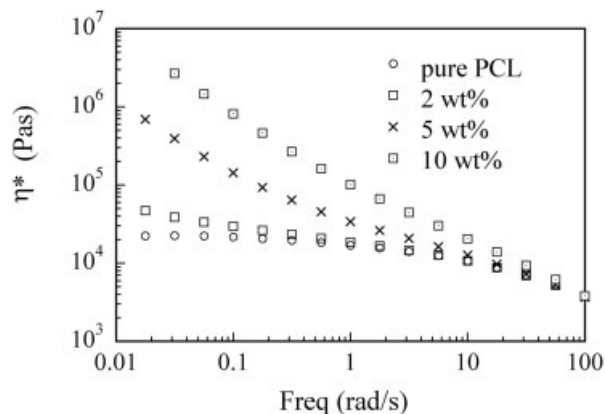


Figure 9. η^* of PCL and PCL/30B nanocomposites with different weight fractions of 30B at 80 °C.

(methyl methacrylate)/clay,²² and polysulfone/organoclay,² and could be partly attributed to the decreased permeability and diffusion of oxygen into the PCL matrix caused by the exfoliated organoclay in the polymer/30B nanocomposites. The enhancement of the thermal stability for nanocomposites also implies improved gas barrier properties with respect to pure PCL, and this is being studied in our laboratory.

Rheological Properties

The complex viscosity (η^*) of the pure PCL and PCL/30B nanocomposites is shown in Figure 9. η^* of the PCL melt shows only a small frequency dependence, with a Newtonian plateau at a low frequency. The effect of the organoclay addition on η^* is very pronounced: η^* of the nanocomposites is higher than that of the neat PCL, and η^* increases with the organoclay content. With more than 2 wt % organoclay, the nanocomposite viscosity curves have a much steeper slope at low frequencies, exhibiting very strong shear thinning behavior. The relative effect diminishes with increasing frequency because of shear thinning. This agrees with experimental observations for PCL and layered silicate nanocomposites synthesized by solution polymerization²³ and other polymer/clay nanocomposites.^{24,25} The increase in η^* with the 30B composition is primarily attributable to the strong interaction between organoclay 30B and PCL molecules.

The strong interaction also caused a dramatic increase in the dynamic shear storage modulus (G') and loss modulus (G'') with respect to those of pure PCL, as can be seen in Figure 10. Both G'

and G'' of the nanocomposites increase with frequency and get close to each other at a high frequency range; however, the rate of increase becomes less at a low frequency range. Therefore, the effect of the 30B concentration is much higher at low frequencies than at high frequencies. It is well known that interacting heterogeneous structures result in an apparent yield stress that is visible in dynamic measurements by a plateau of G' or G'' versus the frequency at low frequencies.²⁶ This effect is more pronounced in G' than in G'' . As the organoclay content increase in such nanocomposite systems, the interaction sites also increase, and a rubberlike interconnected structure will be formed. At about 2 wt % 30B, G' seems to reach such a plateau at a low frequency range. Therefore, an interconnected structure is assumed to form. At higher concentrations of the

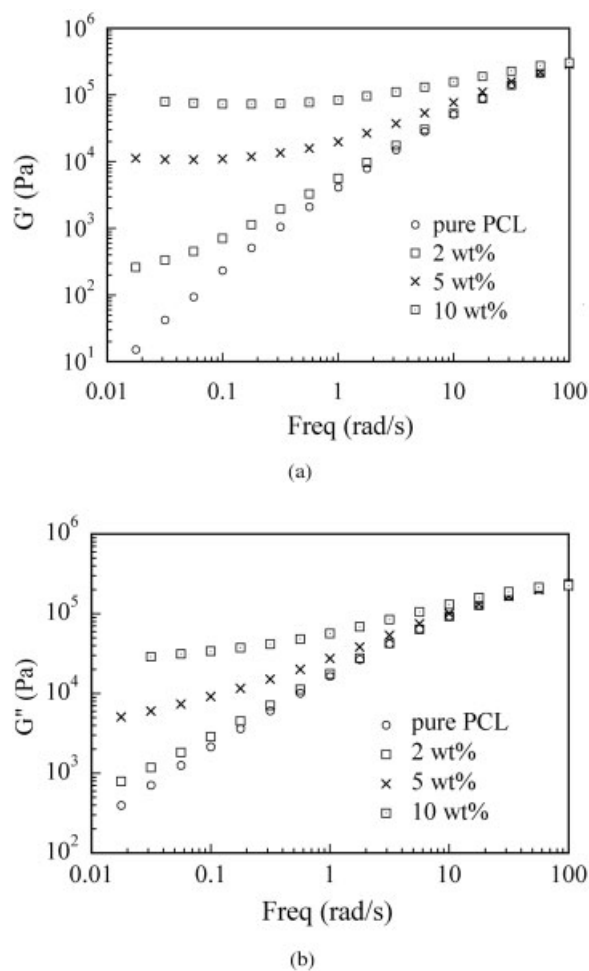


Figure 10. (a) G' and (b) G'' of PCL and PCL/30B nanocomposites with different weight fractions of 30B at 80 °C.

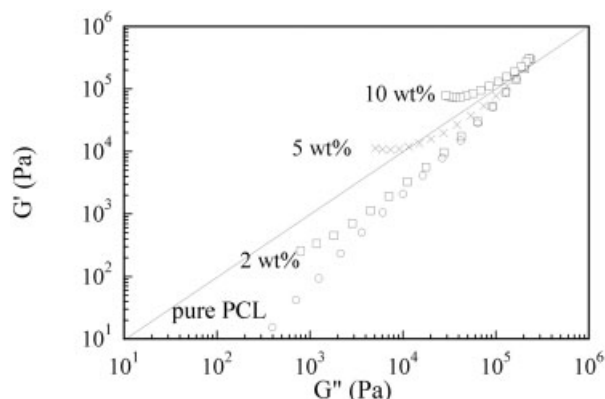


Figure 11. G' as a function of G'' for PCL and PCL/30B nanocomposites with different weight fractions of 30B at 80 °C.

organoclay, the interaction is more pronounced, as seen in the enhanced elasticity in Figure 10.

Figure 11 shows a plot of G' versus G'' for the nanocomposites with frequency as a parameter; it is analogous to Cole–Cole plots used in dielectric spectroscopy.²⁷ Such plots have been used to investigate the structural differences between the matrix and filled systems at a given temperature.²⁸ For the PCL/30B nanocomposites, the slope of G' versus G'' decreases with increasing 30B contents, and G' (for a given G'') increases significantly with increasing contents of 30B. The curves for nanocomposites of different compositions do not fall on the same curve, and this reveals the different structures among them. At contents of 5 wt % and greater, G' is higher than G'' in the low frequency range, and this means they have much longer relaxation times than pure PCL and low 30B content nanocomposites. This shift and the change in the slope of the curves of G' versus G'' also indicate that, with the addition of the organoclay, the microstructure of these nanocomposites changes significantly, and the interaction between the PCL matrix and organoclay increases obviously.²⁹

CONCLUSIONS

The exfoliation of organically modified MMT (organoclay 30B) in a PCL matrix was achieved by melt mixing in an internal mixer. The exfoliation showed a dependence on the type of organic modifier of the organoclay, the organoclay content, and the processing temperature. The strong interaction between the organic surfactants cover-

ing the clay layers and the PCL matrix molecules was favored in the exfoliation process. Processing at low temperatures resulted in high stress in comparison with that at high temperatures, and this helped with the fracturing of the organoclay particles and caused a good dispersion of them in the PCL matrix. A higher organoclay content hybrid required more processing time for achieving an exfoliation structure than a lower organoclay content hybrid.

The well-dispersed organoclay 30B platelets acted as effective nucleating agents in the PCL matrix; however, with an increase in the 30B content, they hindered the movement of PCL molecules, and their crystallization process caused a reduction in the crystallization temperature because of the increased interaction sites between the organic surfactants and PCL molecules. The addition of 30B did not affect the crystal forms and structure, and so the melting point of PCL was not significantly changed. The PCL/30B nanocomposites showed improved thermal stability because the exfoliated platelets retarded the diffusion of oxygen into the polymer matrix. E' was enhanced significantly by the exfoliation of 30B and showed a wider plateau over the experimental temperature range than neat PCL. The dynamic rheological measurements showed much more significant shear-thinning behavior for nanocomposites than the neat PCL melt. G' and G'' exhibited less frequency dependence than pure PCL at a low frequency range. These results have been attributed to the strong interactions of PCL and exfoliated organoclay layers, which lowered the molecular mobility of PCL and the resultant exfoliation structure of the organoclay.

REFERENCES AND NOTES

1. Vaia, R.; Krishnamoorti, R. In *Polymer Nanocomposites*; Krishnamoorti, R.; Vaia, R., Eds.; American Chemical Society: Washington, DC, 2001; Chapter 1, pp 1–7.
2. Sur, G. S.; Sun, H. L.; Lyu, S. G.; Mark, J. E. *Polymer* 2001, 42, 9783.
3. Kojima, Y.; Usuki, A.; Kawasumi, M.; Okada, A. T.; Kamigaito, O. *J Polym Sci Part A: Polym Chem* 1993, 31, 983.
4. Cho, J. W.; Paul, D. R. *Polymer* 2001, 42, 1083.
5. Okamoto, M.; Morita, S.; Taguchi, H.; Kim, Y.; Kotaka, T.; Tateyama, H. *Polymer* 2000, 41, 3887–3890.
6. Yoon, J. T.; Jo, W. H.; Lee, M. S.; Ko, M. B. *Polymer* 2001, 42, 329–336.

7. Liu, X.; Wu, Q. *Polymer* 2001, 42, 10013–10019.
8. Wang, K. H.; Choi, M. H.; Koo, C. M.; Choi, Y. S.; Chung, I. J. *Polymer* 2001, 42, 9819–9826.
9. Lincoln, D. M.; Vaia, R. A.; Wang, Z. G.; Hsiao, B. S. *Polymer* 2001, 42, 1621–1631.
10. Fornes, T. D.; Yoon, P. J.; Keskkula, H.; Paul, D. R. *Polymer* 2001, 42, 9929–9940.
11. Giannelis, E. P.; Krishnamoorti, R.; Manias, E. *Adv Polym Sci* 1999, 138, 107–147.
12. Giannelis, E. P. *Adv Mater* 1996, 8, 29–35.
13. Li, S.; Vert, M. In *Degradable Polymers Principles and Applications*; Scott, G.; Gilead, D., Eds.; Chapman & Hall: London, 1995; Chapter 4, pp 43–87.
14. Messersmith, P. B.; Giannelis, E. P. *J Polym Sci Part A: Polym Chem* 1995, 33, 1047–1057.
15. Kubies, D.; Pantoustier, N.; Dubois, P.; Rulmont, A.; Jérôme, R. *Macromolecules* 2002, 35, 3318–3320.
16. Lepoittevin, B.; Devalckenaere, M.; Pantoustier, N.; Alexandre, M.; Kubies, D.; Calberg, C.; Dubois, P. *Polymer* 2002, 43, 4017–4023.
17. Ho, D. L.; Briber, R. M.; Glinka, C. J. In *Polymer Nanocomposites*; Krishnamoorti, R.; Vaia, R., Eds.; American Chemical Society: Washington, DC, 2001; Chapter 11, pp 127–140.
18. Dennis, H. R.; Hunter, D. L.; Chang, D.; Kim, S.; White, J. L.; Cho, J. W.; Paul, D. R. *Polymer* 2001, 42, 9513–9522.
19. Okamoto, M.; Marita, S.; Kim, Y. H.; Kotaka, T.; Tatehama, H. *Polymer* 2001, 42, 1201.
20. Nam, P. H.; Maiti, P.; Okamoto, M.; Kotaka, T.; Hasegawa, N.; Usuki, A. *Polymer* 2001, 42, 9633–9640.
21. Kodgire, P.; Kalgaonkar, R.; Hambir, S.; Bulakh, N.; Jog, J. *J Appl Polym Sci* 2001, 81, 1786–1792.
22. Lee, D. C.; Jang, L. W. *J Appl Polym Sci* 1996, 61, 1117–1122.
23. Krishnamoorti, R.; Giannelis, E. P. *Macromolecules* 1997, 30, 4097.
24. Solomon, M. J.; Almusallam, A. S.; Seefeldt, K. F.; Somwangthanaroj, A.; Varadan, P. *Macromolecules* 2001, 34, 1864.
25. Krishnamoorti, R.; Silva, A. S. In *Polymer–Clay Nanocomposites*; Pinnavaia, T. J.; Beall, G. W., Eds.; Wiley: New York, 2001; Chapter 15, pp 315–343.
26. Shenoy, A. V. In *Rheology of Filled Polymer Systems*; Kluwer Academic: New Dehli, 1999.
27. Havriliak, J. S.; Havriliak, S. J. In *Dielectric and Mechanical Relaxation in Materials: Analysis, Interpretation and Application to Polymers*; Hanser: Munich, 1997.
28. Poetschlke, T.; Fornes, T. D.; Paul, D. R. *Polymer* 2002, 43, 3247.
29. Han, C. D.; Lem, K. W. *Polym Eng Rev* 1983, 2, 135–165.